Early Events in the Photochemistry of 2-Naphthyl Azide from Femtosecond UV/Vis Spectroscopy and Quantum Chemical Calculations: Direct Observation of a Very Short-Lived Singlet Nitrene

Jin Wang,[†] Jacek Kubicki,[‡] Gotard Burdzinski,[‡] John C. Hackett,[§] Terry L. Gustafson,[†]
Christopher M. Hadad,*[,†] and Matthew S. Platz*[,†]

*Department of Chemistry, The Ohio State University, 100 West 18th Avenue, Columbus, Ohio 43210,
The Quantum Electronics Laboratory, Faculty of Physics, Adam Mickiewicz University,
85 Umultowska, Poznan 61-614, Poland, and Department of Medicinal Chemistry, School of Pharmacy,
Virginia Commonwealth University, Virginia Biotech I, Suite 212, 800 East Leigh Street,
Richmond, Virginia 23219*

hadad.1@osu.edu; platz.1@osu.edu

Received April 24, 2007

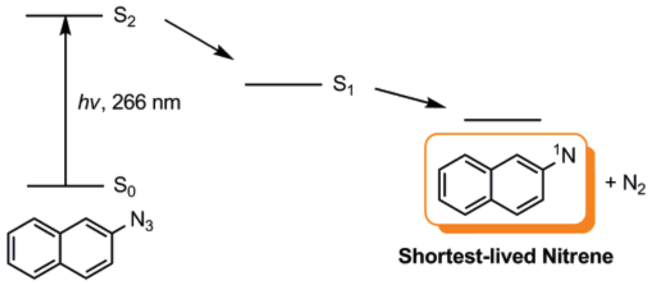

Exposure of 2-naphthyl azide in acetonitrile at ambient temperature to femtosecond pulses of 266 nm light produces a transient absorption with maxima at 350 and 420 nm. The carrier of the 350 nm band decays more rapidly than that of the 420 nm band which has a lifetime of 1.8 ps. Analogous experiments with 1-chloro-2-naphthyl azide in methanol allow the assignment of the 350 nm band to a singlet excited state of 2-naphthyl azide and the carrier of the 420 nm band to singlet 2-naphthylnitrene. This reactive intermediate has the shortest lifetime of any singlet nitrene observed to date and is a true reactive intermediate. Computational studies at the RI-CC2 level of theory support these conclusions and suggest that initial excitation populates the S_2 state of 2-naphthyl azide. The S_2 state, best characterized as a $\pi \rightarrow (\pi^*$, aryl) transition, has a geometry similar to S_0. S_2 of 2-naphthyl azide can then populate the S_1 state, a $\pi \rightarrow$ (in-plane, π^*, azide) excitation, and in the S_1 state, electron density is depleted along the proximal N−N bond. S_1 is dissociative along that N−N coordinate to form the singlet nitrene, and with a barrier of only ~5 kcal/mol for N_2 extrusion.

I. Introduction

Singlet aryl nitrenes have open-shell electronic structures and can be thought of as 1,3-biradicals.[1] For this reason, they rapidly cyclize to form benzazirines in aprotic organic solvents at ambient temperature. Many singlet phenylnitrenes have a lifetime of ~1 ns under these conditions.[1] Recently, we have reported that singlet 1-naphthylnitrene has a lifetime of only 12 ps in acetonitrile at ambient temperature.[2] Theory predicts that the cyclization of singlet 2-naphthylnitrene **^{1}2NN** to

---

[†] The Ohio State University.
[‡] Adam Mickiewicz University.
[§] Virginia Commonwealth University.

(1) (a) Gritsan, N. P.; Platz, M. S. *Adv. Phys. Org. Chem.* **2001**, *36*, 255. (b) Platz, M. S. Nitrenes. In *Reactive Intermediate Chemistry*; Moss, R. A., Platz, M. S., Jones, M., Jr., Eds.; Wiley: New York, 2004; pp 501−560. (c) Schuster, G. B.; Platz, M. S. Photochemistry of Phenyl Azide. In *Advances in Photochemistry*; Volman, D., Hammond, G., Neckers, D., Eds.; Wiley: New York, 1992; Vol. 17, pp 69−143.

(2) (a) Burdzinski, G.; Gustafson, T. L.; Hackett, J. C; Hadad, C. M.; Platz, M. S. *J. Am. Chem. Soc.* **2005**, *127*, 13764. (b) Burdzinski, G.; Hackett, J. C; Wang, J.; Gustafson, T. L.; Hadad, C. M.; Platz, M. S. *J. Am. Chem. Soc.* **2006**, *128*, 13402.

10.1021/jo070865w CCC: $37.00

SCHEME 1

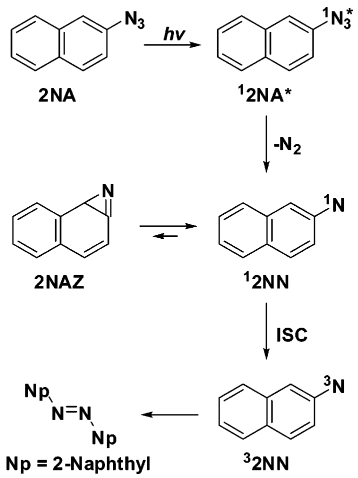

naphthazirine **2NAZ** (Scheme 1) involves a much lower barrier than the corresponding reaction of singlet 1-naphthylnitrene (3.02 versus 5.53 kcal/mol).[3] Given the small barrier heights and uncertainties in the level of theory used for these calculations, it is not clear whether or not **^{1}2NN** even exists with a finite lifetime. In fact, nanosecond laser flash photolysis (LFP) of 2-naphthyl azide at 77 K *fails* to provide any evidence for the existence of **^{1}2NN**, unlike the case with singlet 1-naphthylnitrene,[2] suggesting a picosecond lifetime or shorter for **^{1}2NN**, even at 77 K.[4] Nanosecond LFP at ambient temperature produces the IR spectrum of naphthazirine **2NAZ** (1724 cm^{-1}), and this species has a lifetime of 150 ± 10 μs.[4]

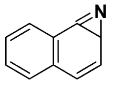

1NAZ

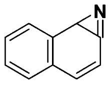

2NAZ

Theory predicts that cyclization of singlet 2-naphthylnitrene is exothermic by 3−4 kcal/mol, whereas cyclization of 1-naphthylnitrene to 1-naphthazirine (**1NAZ**) is predicted to be thermoneutral.[3] Calculations indicate further that **1NAZ** and **2NAZ** differ in energy by only 0.46 kcal/mol with **1NAZ** favored, but that singlet 1-naphthylnitrene is 4.48 kcal/mol more stable than singlet 2-naphthylnitrene.[3] This explains the greater intramolecular reactivity of the higher energy isomer, **^{1}2NN**. Nanosecond time-resolved laser flash photolysis (LFP) experiments have demonstrated that singlet 2-naphthylnitrene must cyclize with a rate constant $\gg 1.1 \times 10^7$ s^{-1} at 77 K. Assuming a normal Arrhenius pre-exponential *A* factor of 10^{13} s^{-1} for cyclization, one concludes that the barrier to isomerization of **^{1}2NN** must be less than 2.1 kcal/mol.[4]

The naphthazirines equilibrate with the isomeric singlet naphthylnitrenes which eventually relax by intersystem crossing (ISC) to the lower energy triplet nitrenes. The triplet nitrenes can then dimerize (Scheme 1) to form azo compounds. Shrock and Schuster observed only the slow formation of azo dimer by nanosecond time-resolved LFP of 2-naphthyl azide in benzene solution at ambient temperature with UV−Vis detection.[5]

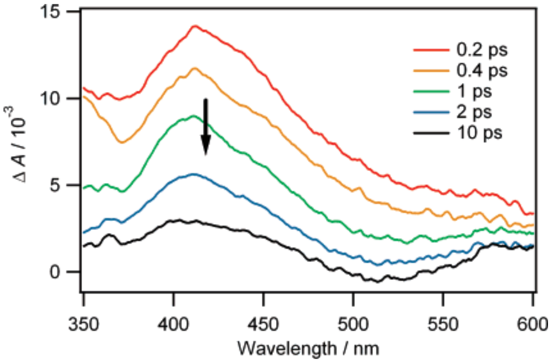

FIGURE 1. Transient absorption spectra produced by 266 nm photolysis of 2-naphthyl azide in acetonitrile at ambient temperature with a time window of 0.2−10 ps.

Herein, we report ultrafast time-resolved studies of the photochemistry of 2-naphthyl azide. Singlet 2-naphthylnitrene has been directly observed for the first time, and it has a lifetime of only 1.8 ps in acetonitrile at ambient temperature. It is a true reactive intermediate, although it has the shortest lifetime in solution of any singlet nitrene studied to date. We also support the experimental studies with computational investigations of the excited state potential energy surfaces.

II. Results and Discussion

II.1. Ultrafast Spectroscopic Studies of 2-Naphthyl Azide. Ultrafast LFP (λ_{ex} = 266 nm) of 2-naphthyl azide in acetonitrile produces the transient spectrum of Figure 1. Transient absorption bands centered at 350 and 420 nm are formed within the time resolution of the spectrometer (300 fs). At longer delay times (>1 ps), only transient absorption at 420 nm is observed. The carrier of the 350 nm band has a shorter lifetime than that of the 420 nm peak, thus we must be detecting the transient absorption of at least two distinct species whose spectra overlap severely. The lifetime of the species absorbing at 420 nm is 1.8 ps (Figure 2). The lifetime of the carrier of the 350 nm transient absorption is within the instrument response (300 fs). Similar time constants were obtained in methanol (Supporting Information (SI), Figure S1).

CASSCF calculations predict that **^{1}2NN** will absorb strongly at 523, 452, and 342 nm.[4] Tsao's CASPT2 calculations predicted that **^{1}2NN** will absorb at 677, 516, 421, 412, and 363 nm, and these results also seem to fit the 350 and 420 nm absorbing transients equally well.[4] The calculated oscillator strengths do not aid further in the assignment of the carrier of the transient spectra of Figure 1. Thus, another approach must be used to assign the experimental spectra.

II.2. Ultrafast Spectroscopic Studies of 1-Chloro-2-naphthyl Azide. The rate of cyclization of a singlet arylnitrene is modulated by both steric and electronic effects.[1] The lifetime of singlet 2-biphenylylnitrene (λ_{max} = 400 nm) is 16 ps in acetonitrile at ambient temperature, for example.[2] Ultrafast LFP of 2-azido-3,5-dichlorobiphenyl produces the expected nitrene (λ_{max} = 425 nm in cyclohexane).[6] The lifetime of singlet 3,5-dichloro-*ortho*-biphenylylnitrene is 260 ps in cyclohexane and is only 62 ps in methanol (Scheme 2). The chlorine substituent lengthens the lifetime of the singlet nitrene without significant alteration of the absorption spectrum of the nitrene.[2,6] One does

---

(3) Maltsev, A.; Bally, T.; Tsao, M. L.; Platz, M. S.; Kuhn, A.; Vosswinkel, M.; Wentrup, C. *J. Am. Chem. Soc.* **2004**, *126*, 237.

(4) Tsao, M.-L.; Platz, M. S. *J. Phys. Chem. A* **2004**, *108*, 1169.

(5) Schrock, A. K.; Schuster, G. B. *J. Am. Chem. Soc.* **1984**, *106*, 5234.

(6) Gritsan, N. P.; Polshakov, D. A.; Tsao, M. L.; Platz, M. S. *Photochem. Photobiol. Sci.* **2005**, *4*, 23.

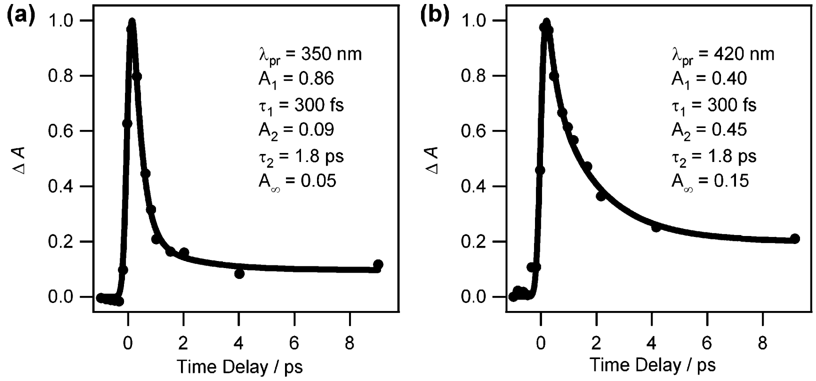

FIGURE 2. Normalized kinetic traces of photolysis (λ_{ex} = 266 nm) of 2-naphthyl azide in acetonitrile at ambient temperature. The kinetic traces are probed at (a) 350 nm and (b) 420 nm and globally fitted in biexponential functions with deconvolution of instrument response function (300 fs).

SCHEME 2

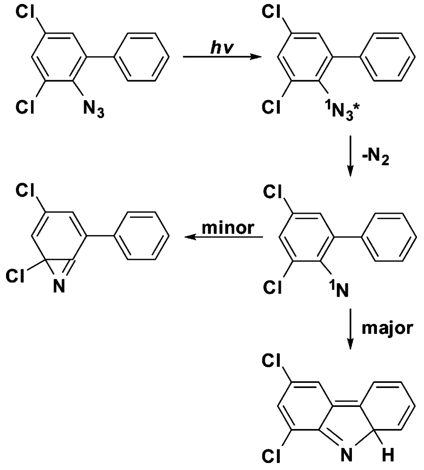

SCHEME 3

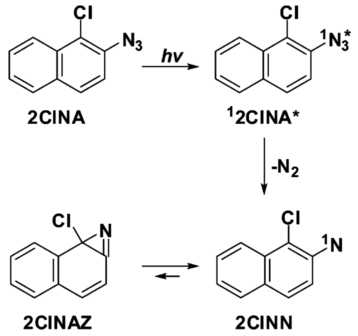

not expect that the chlorine substituent will alter the spectrum of 2-naphthylnitrene. Thus, 1-chloro-2-naphthyl azide (**2ClNA**) was synthesized and studied by ultrafast time-resolved spectroscopic techniques (Scheme 3).

Ultrafast photolysis (λ_{ex} = 308 nm) of 1-chloro-2-naphthyl azide in methanol[7] produces the transient spectrum shown in Figure 3. There is a small weak absorption band present at 370 nm and a more intense band at 420 nm with a shoulder at ~520 nm. The decay of transient absorption at 370 and 520 nm results in a growth of transient absorption at 420 nm, with isosbestic points at 380 and 460 nm. The latter bands narrow over 5 ps, as a result of vibrational cooling[8] and then

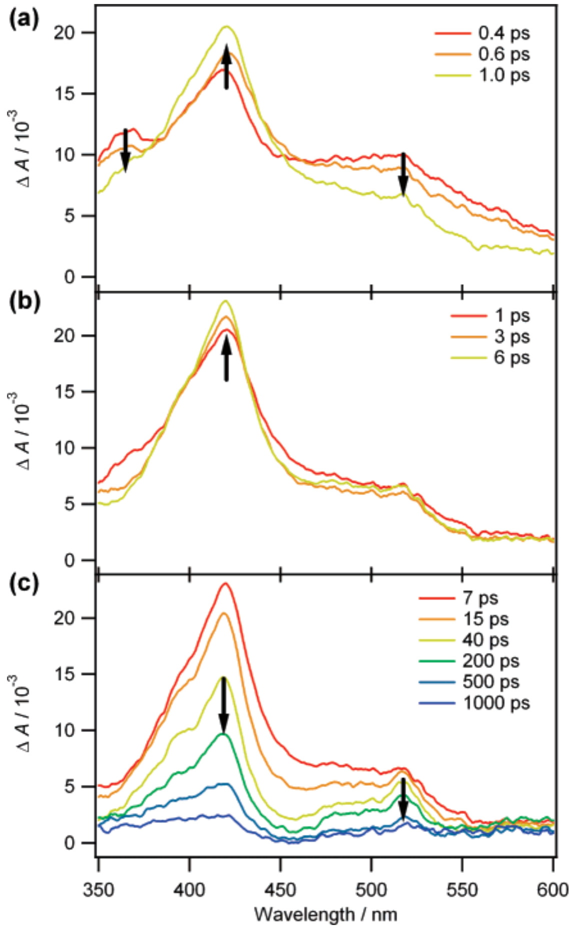

FIGURE 3. Transient absorption spectra produced by 308 nm photolysis of 1-chloro-2-naphthyl azide in methanol at ambient temperature. The transient spectra were recorded in time windows of (a) 0.4–1.0 ps, (b) 1–6 ps, and (c) 7–1000 ps.

---

[7] Photolysis of 1-chloro-2-naphthyl azide in acetonitrile produced spots (precipitates) preventing study in this solvent. In addition, although spectrophotometric grade methanol from Burdick & Jackson was used, pure methanol solvent will produce significant signals at longer delays (>100 ps) at 270 nm excitation, which may be due to some unknown impurities. Considering these two reasons, photolysis of 1-chloro-2-naphthyl azide was conducted in methanol using 308 nm excitation.

[8] (a) Laermer, F.; Elsaesser, T.; Kaiser, W. *Chem. Phys. Lett.* **1989**, *156*, 38. (b) Miyasaka, H.; Hagihiro, M.; Okada, T.; Mataga, N. *Chem. Phys. Lett.* **1992**, *188*, 259. (c) Schwarzer, D.; Troe, J.; Votsmeier, M.; Zerezke, M. *J. Chem. Phys.* **1996**, *105*, 3121. (d) Elsaesser, T.; Karser, W. *Annu. Rev. Phys. Chem.* **1991**, *42*, 83.

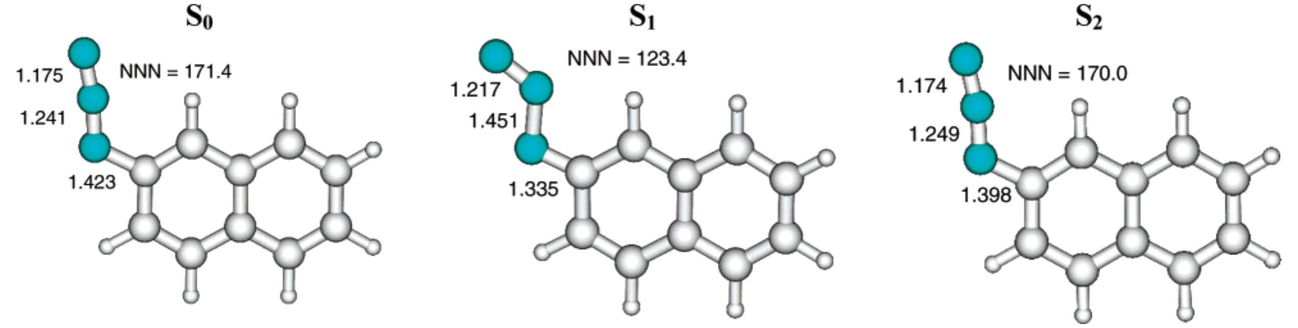

FIGURE 4. RI-CC2/TZVP 2-naphthyl azide ground and excited state equilibrium geometries. Bond distances and angles are listed in angstroms and degrees, respectively.

decay over hundreds of picoseconds (SI, Figure S2). As the 1-chloro substituent is expected to lengthen only the nitrene lifetime, we assign the carriers of the 420 and 520 nm transient absorption to singlet 1-chloro-2-naphthylnitrene, and by extension, we assign the carrier of 420 nm absorption in Figure 1 to singlet 2-naphthylnitrene. This species (**^{1}2NN**) is the shortest-lived nitrene ever observed ($\tau = 1.8$ ps). The excited state of the azide **^{1}2ClNA*** likely has some absorbance at 370 and 520 nm which accounts for the fast (fs) decay component observed at these wavelengths.

II.3. Computational Chemistry: Ground State Equilibrium Geometries, Vertical Excitation Energies, and Difference Densities. We have applied resolution-of-the-identity coupled cluster (RI-CC2)[9] and time-dependent density functional theory (TD-DFT)[10] methods to explore the different energy surfaces for the ground and excited states of these azides and nitrenes. In our recent reports, we have shown the value of these methods for understanding the ultrafast spectroscopy of aryl azides.[2] For our DFT computations, we have utilized the B3LYP density functional.[11]

The singlet ground (S_0), first excited (S_1), and second excited (S_2) states of **2NA** (Figure 4) were optimized at the RI-CC2 and B3LYP levels of theory. **2NA** was optimized with C_s (planar) symmetry. (Optimizations performed without symmetry restraints remained C_s symmetric, and therefore only the results obtained with C_s species will be described here.) Vertical excitation energies, oscillator strengths, and the dominant occupied and virtual orbitals contributing to the lowest energy singlet excitations are listed in Table 1. Contour surfaces for these orbitals are presented in the Supporting Information.

Vertical transitions to the first and second excited states are very similar in energy, and both states could be populated by 266 nm photolysis of the azide precursor (Table 1). Inspection of the Kohn−Sham orbitals resulting from B3LYP density functional theory calculations reveal the second excited state (S_2) is characterized by a $\pi \rightarrow$ (π*, aryl) transition in which the π* orbital is localized on the aryl ring, whereas the first excited state (S_1) is characterized by a $\pi \rightarrow$ (in-plane, π*, azide) orbital transition in which the π* orbital is localized on the azide unit. In contrast, at the RI-CC2 level of theory, the ordering of these states is reversed, in which the vertical $\pi \rightarrow$ (π*, aryl) transition is lower in energy relative to the $\pi \rightarrow$ (in-plane, π*, azide) transition by only 0.05 eV. Obviously, the energetic ordering is very similar between the two states, and moreover, both states can be readily excited experimentally by the 266 nm excitation. Additionally, the a″ orbitals involved in the lowest-lying RI-CC2 $\pi \rightarrow$ (π*, aryl) excited state are somewhat different compared to B3LYP but, nevertheless, localized to the naphthyl unit (Supporting Information). This difference in the excited state ordering may be attributed to limitations of using the RI-CC2 ground state geometry, and furthermore, when these excited states are fully optimized using RI-CC2, the $\pi \rightarrow$ (in-plane, π*, azide) state drops below the $\pi \rightarrow$ (π*, aryl) state as computed by TD-B3LYP (vide infra). In the remaining discussion, S_1 and S_2 refer to the $\pi \rightarrow$ (in-plane, π*, azide) and the $\pi \rightarrow$ (π*, aryl) states, respectively. Additionally, these transitions have multiconfigurational character, electron redistribution as a result of excitation requires consideration of the total electron densities for the ground and excited states.

TABLE 1. TD-B3LYP and RI-CC2 Vertical Excitation Energies, Oscillator Strengths, and the Dominant Occupied and Virtual Orbitals Contributing to the Two Lowest Energy Singlet Excitations of 2-Naphthyl Azide[a]

state	character (% contribution)	energy/eV (nm)	oscillator strength
	TD-B3LYP/TZVP[b]		
S_1	$7a'' \rightarrow 38a'$ (85%)	3.78 (328)	1.82×10^{-4}
S_2	$7a'' \rightarrow 8a''$ (79%)	3.04 (307)	7.38×10^{-2}
S_3	$6a'' \rightarrow 8a''$ (49%) $7a'' \rightarrow 9a''$ (35%)	4.20 (295)	9.80×10^{-3}
	RI-CC2/TZVP[c]		
S_1	$6a'' \rightarrow 8a''$ (40%) $7a'' \rightarrow 9a''$ (39%)	4.26 (291)	1.98×10^{-2}
S_2	$7a'' \rightarrow 38a'$ (50%)	4.31 (288)	4.56×10^{-4}
S_3	$7a'' \rightarrow 8a''$ (76%)	4.72 (263)	9.51×10^{-2}

[a] Transitions to the excitation contributing to ≥30% are listed. [b] Using the B3LYP/TZVP optimized geometry for the S_0 state. [c] Using the RI-CC2/TZVP optimized geometry for the S_0 state.

One can visualize such electron redistribution by the use of a difference density between the excited and the ground state (using the S_0 geometry). The difference densities at the RI-CC2 level for the first (S_1) and second (S_2) excited states relative to the ground state are depicted in Figure 5 for **2NA**. In those figures, green contours correspond to electron density being accumulated in the excited state, and red contours correspond to electron density being depleted from S_0. Difference densities of the second excited states reveal a redistribution of electron density, which is localized to the aryl's π system and for which there is no appreciable change in electron density for the azide moiety. In contrast, electron redistribution in the first excited state is characterized by a depletion of electron density from

---

(9) Hättig, C.; Weigend, F. *J. Chem. Phys.* **2000**, *113*, 5154.

(10) (a) Furche, F.; Ahlrichs, R. *J. Chem. Phys.* **2002**, *117*, 7433. (b) Furche, F.; Ahlrichs, R. *J. Chem. Phys.* **2004**, *121*, 12772.

(11) (a) Becke, A. D. *Phys. Rev. A* **1988**, *38*, 3098. (b) Becke, A. D. *J. Chem. Phys.* **1993**, *98*, 5648. The version of the B3LYP density functional used includes VWN-V rather than VWN-III.

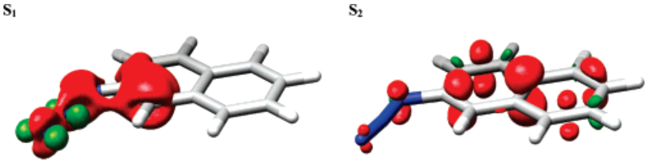

FIGURE 5. RI-CC2/TZVP excited state difference density plots (S_1 and S_2 densities less the ground state density) for 2-naphthyl azide. A red surface surrounds areas where electron density is depleted from S_0; a green surface surrounds areas where electron density is accumulated in the excited state. S_1 and S_2 plots are plotted with isocontour values of ±0.02 and ±0.005 au, respectively.

the in-plane aryl azide's π system and in the region of the N−N bond proximal to the naphthalene unit. Loss of electron density in the proximal N−N bonding region is consistent with expulsion of N_2 in the first excited state, as will be discussed later. (TD-B3LYP difference densities are presented in the Supporting Information.)

II.4. Computational Chemistry: Excited State Equilibrium Geometries and Potential Energy Surfaces. Using the recent implementation of RI-CC2 analytical gradients for excited states, the equilibrium geometries for the first and second excited states of **2NA** were computed. Attempts to optimize the excited states' geometries using time-dependent density functional theory at the TD-B3LYP level failed due to instabilities in the DFT reference wave function as the proximal N−N bond lengthened in the first excited state. We noted similar difficulties earlier with other aryl azides.[2] Therefore, the discussion here will be limited to the RI-CC2 results.

Equilibrium geometries of the first and second excited states are displayed in Figure 4. With the exception of modest changes in bond lengths, the geometrical parameters of the second excited state (S_2) of 2-naphthyl azide are similar to those of the ground state (S_0). In contrast, the first excited state (S_1) is characterized by a remarkable lengthening of the proximal N−N bond and bending of the azide group. **2NA** has a proximal N−N bond length of ∼1.45 Å in the S_1 state, ∼0.2 Å longer than for the S_0 ground state. The lengthening of the proximal N−N bond is consistent with the depletion of electron density in this region as observed in the excited states' difference density plots (see Figure 5). **2NA** has a significantly bent N−N−N angle of 123° in the S_1 state, also quite different from the 171° bond angle in the S_0 state.

Furthermore, given the electronic redistribution that occurred in the first excited state as well as the lengthening of the proximal N−N bond, we hypothesized that the first excited state may be dissociative to form molecular nitrogen and the corresponding singlet arylnitrene. We performed a fully relaxed potential energy surface scan of the N−N coordinate in **2NA** (Figure 6). In general, the features of the ground and excited states' potential energy surfaces are similar to those obtained from **1NA**.[2] The barrier for expulsion of N_2 on the S_0 surface is ∼54 kcal/mol. On the S_2 surface, the barrier for N_2 expulsion is ∼40 kcal/mol, similar to the value computed for the S_0 surface. The fully relaxed scan of the N−N coordinate on the S_1 surface further supports the hypothesis that this state is dissociative. The barrier for N_2 expulsion on the S_1 surface is only ∼5 kcal/mol. The S_0/S_1 state crossing occurs at a N−N distance of ∼1.8 Å. A very interesting feature of the fully relaxed S_1 potential energy surface (Figure 6) is the presence of an intersection with the S_2 surface near ∼1.1 Å. Thus, it appears that S_2 can couple vibronically to S_1 near the S_0 geometry, thus providing a route for decay of the electronically excited S_2 state to the lower energy S_1 surface.

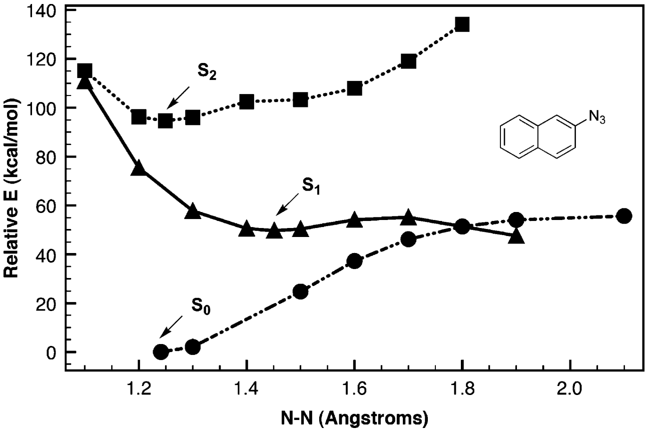

FIGURE 6. RI-CC2/TZVP fully relaxed potential energy curves for N_2 expulsion from 2-naphthyl azide. Ground state (●), first excited state (▲), and second excited state (■). The arrows indicate the N−N bond length of the fully optimized stationary point on each respective potential energy surface.

The TD-B3LYP calculations (Table 1) predict that the transition of S_0 to S_2 has a much larger oscillator strength than the S_0 to S_1 transition in **2NA**, but both S_1 and S_2 states should be accessible by 266 nm photolysis. Thus, UV excitation is predicted to promote the ground state azide to the S_2 state, and the S_2 state undergoes only a small geometric distortion relative to S_0. Internal conversion of the S_2 state to the S_1 state can then occur at a short proximal N−N distance. The S_1 state of the azide will then undergo nitrogen extrusion by extension of the N−N bond, and with a small barrier of ∼5 kcal/mol. This process is highly exothermic (47 kcal/mol at the B3LYP/TZVP level of theory for **2NA**), and consequently, a vibrationally excited 2-naphthylnitrene will be formed. The S_1 state of the azide may also deactivate to the ground state via the S_0/S_1 state crossing or through a S_0/S_1 conical intersection analogous to that identified for phenyl azide,[2] thereby reducing the efficiency of arylnitrene formation.

III. Conclusions

We have previously reported that nanosecond (ns) laser flash photolysis of 1-naphthyl azide in a clear glass at 77K produces the transient spectrum of singlet 1-naphthylnitrene which has a lifetime of 91 ns under these conditions. The analogous ns LFP experiments with 2-naphthyl azide failed to produce spectroscopic evidence for singlet 2-naphthylnitrene. Those results were consistent with calculations which predicted that singlet 2-naphthylnitrene would cyclize to an azirine faster than the 1-naphthyl isomer. In fact, it is not clear from those calculations whether or not singlet 2-naphthylnitrene is a species which corresponds to a minimum on a potential energy surface and would have a finite lifetime.

However, ultrafast photolysis of 2-naphthyl azide at ambient temperature produces transient spectra with maxima at 350 and 420 nm. The carrier of transient absorption at 350 nm decays more rapidly than that of 420 nm which has a lifetime of 1.8 ps. Our previous work with 2-biphenylylnitrene revealed that an appropriately placed chlorine substituent will extend the lifetime of a singlet nitrene without significant alteration of its spectrum. Thus, we synthesized 1-chloro-2-naphthyl azide reasoning that the chlorine substituent would not significantly alter the spectrum of the nitrene, but would dramatically extend its lifetime. Ultrafast photolysis of 1-chloro-2-naphthyl azide produces transient spectra with maxima at 370, 420, and 520 nm. The carrier of transient absorption at 370 nm and the fast component of the decay recorded at 520 nm have lifetimes of 0.8 ps and are both assigned to the azide excited state. The lifetime of transient absorption at 420 nm and the slow component of 520 nm decay have lifetimes of 500 ps and are attributed to the singlet nitrene. This analysis of the 1-chloro-2-naphthyl azide spectra allows us to assign the 350 nm band produced by photolysis of 2-naphthyl azide to the excited state of the azide and the 420 nm band to singlet 2-naphthylnitrene. The latter species has a lifetime of 1.8 ps which is the shortest lifetime of any singlet nitrene currently known.

Computational studies at the RI-CC2 level of theory support these conclusions, and suggest that initial excitation populates the S_2 state of 2-naphthyl azide. The S_2 state, best characterized as a $\pi \rightarrow (\pi^*$, aryl) transition, has a similar geometry to S_0. S_2 of 2-naphthyl azide can then populate the S_1 state, a $\pi \rightarrow$ (in-plane, π^*, azide) excitation, and electron density is depleted along the proximal N−N bond. S_1 is dissociative along the proximal N−N coordinate to form the arylnitrene, and with a barrier of only ~5 kcal/mol for N_2 extrusion. At this time, we are unable to assign the excited state we have experimentally observed to either S_1 or S_2. This assignment awaits ultrafast time-resolved vibrational spectroscopic analysis.

IV. Experimental and Computational Methods

IV.1. Computational Methods. Geometry optimizations were performed with the TURBOMOLE 5.71 suite of programs for electronic structure calculations.[12,13] The geometries of the ground states were optimized using the approximate second-order coupled-cluster wave function model using the resolution-of-the-identity approximation (RI) for the electron repulsion integrals (RI-CC2) and with the hybrid density functional, B3LYP. In the RI-CC2 calculations, a frozen-core approximation was employed in which the 1s electrons of C and N atoms were excluded from the correlation treatment. The TZVP ([11s6p1d]/[5s3p1d] for C, N and [10s]/[4s] for H) basis sets of Ahlrichs and co-workers[14,15] were used for all calculations. The equilibrium geometries for the excited states were optimized using recent implementations of analytical gradients for RI-CC2[16,17] and time-dependent density functional theory (TD-DFT) in TURBOMOLE.

IV.2. Femtosecond Broad-Band UV−Vis Transient Absorption Spectrometer. Ultrafast UV−Vis broad-band absorption measurements were performed using the home-built spectrometer described previously.[2b] Samples were prepared in 50 mL of solvent with an optical absorption of ~1.0 at the chosen excitation wavelength and using a 1.0 mm optical path length.

IV.3. Materials. 2-Naphthyl azide has been previously reported and was synthesized and purified by the methods described elsewhere.[1] Acetonitrile and methanol (spectrophotometric grade) were used as received.

1-Chloro-2-naphthyl Azide. 1-Chloro-2-naphthylamine was prepared following the literature procedure[18] and used without further purification. 1-Chloro-2-naphthylamine (1.24 g, 7.0 mmol) was dissolved in 5 mL of THF. Forty-five milliliters of 5% HCl was added, and the solution was cooled to −5 °C and stirred for 15 min. Twenty milliliters of $NaNO_2$ solution (1.4 g of $NaNO_2$ in 20 mL of water) was then added dropwise to the solution and stirred for another 15 min. A spatula of urea was added to remove the excess acid. Then 20 mL of NaN_3 solution (1.8 g of NaN_3 in 20 mL of water) was added dropwise. After the addition of NaN_3 solution, precipitate formed and the reaction was kept in the freezer overnight. Filtration afforded dark brown crude. The crude was recrystallized in pentane to give 0.71 g (yield 50%) of wine-red needle crystals: ^1H NMR (500 MHz, $CDCl_3$) δ 8.23 (d, $J = 9.1$ Hz, 1H), 7.84−7.80 (m, 2H), 7.62 (ddd, $J = 8.4, 6.9, 1.2$ Hz, 1H), 7.50 (ddd, $J = 8.1, 6.9, 1.1$ Hz, 1H), 7.34 (d, $J = 8.8$ Hz, 1H); ^{13}C NMR (125 MHz, $CDCl_3$) δ 134.0, 131.7, 131.6, 128.4, 128.2, 128.1, 126.0, 124.3, 120.4, 117.5; FT-IR (neat) 2114 cm^{-1}; UV λ_{max} (acetonitrile) 215, 250, 291, 300 (shoulder) nm.

Acknowledgment. This work was performed at The Ohio State University Center for Chemical and Biophysical Dynamics (CCBD). Generous computational resources at the Ohio Supercomputer Center are gratefully acknowledged. Financial support of this work, and of the CCBD, by the National Science Foundation is gratefully acknowledged. J.W. thanks the Ohio State University Graduate School for a Presidential Fellowship. G.B. is a holder of a “Homing” grant from the Foundation for Polish Science (FNP) in the year 2007. The authors gratefully acknowledge a suggestion by Professor W.T. Borden which promoted our study of 1-chloro-2-naphthyl azide.

Supporting Information Available: Ultrafast LFP kinetic traces of 2-naphthyl azide and 1-chloro-2-naphthyl azide in methanol and additional computational data are included in Supporting Information. This material is available free of charge via the Internet at http://pubs.acs.org.

JO070865W

---

[12] (a) Ahlrichs, R.; Bär, M.; Häser, M.; Horn, H.; Kölmel, C. *Chem. Phys. Lett*. **1989**, *162*, 165. (b) For the current version of TURBOMOLE, see http://www.turbomole.de.

[13] Treutler, O.; Ahlrichs, R. *J. Chem. Phys.* **1995**, *102*, 346.

[14] Schäfer, A.; Huber, C.; Ahlrichs, R. *J. Chem. Phys.* **1994**, *100*, 5829.

[15] Eichkorn, K.; Weigend, F.; Treutler, O.; Ahlrichs, R. *Theor. Chem. Acc.* **1997**, *97*, 119.

[16] Hättig, C.; Weigend, F. *J. Chem. Phys*. **2000**, *113*, 5154.

[17] Hättig, C.; Köhn, A. *J. Chem. Phys*. **2002**, *117*, 6939.

[18] Markgraf, J. H.; Davis, H. A.; Ernst, P. S.; Hirsch, K. S.; Leonard, K. J.; Morrison, M. E.; Myers, C. R. *Tetrahedron* **1991**, *47*, 183.